Table III. Atomic Parameters Used in the Calculations

orbital		H_{ii}, eV	ζ_1	ζ_2	c_1[a]	c_2[a]
U	7s	-5.51	1.91			
	7p	-5.51	1.91			
	6d	-5.12	2.58	1.21	0.7608	0.4126
Gd	6s	-7.67	2.14			
	6p	-5.01	2.08			
	5d	-8.21	3.78	1.38	0.7765	0.4587
Co	4s	-9.21	2.00			
	4p	-5.29	2.00			
	3d	-13.18	5.55	2.10	0.5680	0.6060
C	2s	-21.40	1.62			
	2p	-11.40	1.62			
Ca	4s	-7.00	1.20			
	4p	-4.00	1.20			

[a] Double ζ expansion coefficients of the orbitals.

co-workers, silicide analogues of such carbides are unlikely to be synthesized, because of the high coordination number (8 if there is no short C-C contact as in $ThCr_2Si_2$) around small carbon atoms.[18] They propose an alternative structure, a $ThCr_2Si_2$ type carbide with singly bonded carbon pairs, which may be particularly favorable for large, electropositive divalent metals. To see how the two structures differ electronically, we have performed a series of calculations using the two models described below: (I) a carbide of $ThCr_2Si_2$ type with carbon-carbon bonds of 1.50 Å and M-C separation of 2.47 Å and (II) a $ThCr_2Si_2$ metal-carbon structure with eight-coordinated carbon atoms, where the M-C bond is taken the same as in $UCoC_2$ and the C-C distance is a long 2.5 Å. Calculated total average energies for electron counts of 22-32 are listed in Table II. It seems that structure II continues to be preferred for lower electron counts. Such a preference is lost only for counts of 29 or more electrons in which case structure I becomes more favorable. Since one of the two carbon atoms in the 2c positions of a $UCoC_2$ structure is already 8-coordinated to uranium and cobalt, it seems not too unreasonable to think of configuration II as a candidate for carbides of RT_2C_2 composition by making the other carbon also eight-coordinated upon addition of a transition-metal square lattice to the $UCoC_2$.

Acknowledgment. This work is supported by the National Science Foundation through Research Grant CHE 8406119. J.L. would like to thank Marja Zonnevylle for some helpful suggestions. We are grateful to Jane Jorgensen and Elisabeth Fields for the drawings.

Appendix

An extended Hückel tight-binding approach is employed throughout this paper. Atomic parameters used in the calculations were taken from previous work[94] and are tabulated in Table III. Geometrical data for the UC_2, CaC_2, $DyCoC_2$, and $UCoC_2$ structure were obtained from reported X-ray crystallographic experimental results. Gd parameters were used for the Dy atoms. Several k-point sets were used in calculations of average properties. These were chosen according to the Pack and Monkhorst method[95a] as well as to the Ramirez and Böhm method.[95b]

(94) (a) Ortiz, J. V.; Hoffmann, R. *Inorg. Chem.* **1985**, *24*, 2095. Tatsumi, K.; Nakamura, A. *J. Am. Chem. Soc.* **1987**, *109*, 3195. (b) 68. (c) Summerville, R. H.; Hoffmann, R. *J. Am. Chem. Soc.* **1976**, *98*, 7240. (d) 69(a). (e) Zheng, C.; Hoffmann, R. *J. Am. Chem. Soc.* **1986**, *108*, 3078.

(95) (a) Pack, J. D.; Monkhorst, H. J. *Phys. Rev.* **1977**, *B16*, 1748. (b) Ramirez, R.; Böhm, M. C. *Int. Quantum Chem.* **1986**, *30*, 391.

Angularly Resolved Second Harmonic Generation Study of the Air-Formed Oxide on Iron

M. W. Schauer, M. J. Pellin, and D. M. Gruen*

Materials Science and Chemistry Divisions, Argonne National Laboratory, Argonne, Illinois 60439

Received August 8, 1988

By variance of the angle of incidence and input polarization, it is possible to obtain structural information about the oxide layer that forms on iron surfaces from angularly resolved second harmonic generation (AR-SHG) experiments. The AR-SHG experiments on air-oxidized (110) iron single-crystal surfaces reveal the presence of both 2-fold and 3-fold symmetric species at the metal/oxide interface. These patterns are fit to an extension of existing theory, and the 3-fold symmetric oxide is found to be tilted by about 5° from the Fe (110) plane. The 2-fold symmetric structure is aligned with the Fe (110) surface, and the SHG intensity contains both surface and bulk contributions.

Introduction

Structural information about the oxides that form on iron surfaces is crucial to the understanding of corrosion and passivation. The understanding of these phenomena has motivated innumerable studies since the discovery of the passive oxide layer on iron.[1] Much has been learned about the possible composition of the passive film that forms on iron and other metals, yet despite extensive study, the chemical and structural details of this very important system remain largely a mystery.

One of the unique capabilities of second harmonic generation (SHG) as a surface analytical tool is the ability to probe a solid-solid interface below the surface of a material. The dipolar contribution to the induced polarization in the medium that gives rise to the SHG signal is necessarily zero in bulk, isotropic material. Therefore, the major contribution to the signal in an SHG experiment arises near an interface, where the bulk symmetry is broken.

The tensorial nature of the second-order nonlinear susceptibility that governs SHG can be used to obtain structural information about an interface. The symmetry

(1) *Passivity of Metals*; Frankenthal, R. P., Kruger, J., Eds.; The Electrochemical Society: Princeton, NJ, 1978.

0897-4756/89/2801-0101$01.50/0

of a single-crystal surface can be observed by monitoring the SHG intensity as the crystal surface is rotated about its normal. The use of various input angles and polarizations in many cases allows a fairly complete description of the symmetry of an interface. The symmetry of metal and semiconductor surfaces has been observed in ultrahigh vacuum (UHV) environments, with and without adsorbates.[2-10] Also, the symmetry of a silver electrode in an electrochemical cell has been monitored as electrochemical processes occur.[11-18] These studies have demonstrated the capability of SHG experiments to uncover the structure of an interface.

A sharp compositional change below a solid surface can also be probed as long as it is within the evanescent wave of the beam that is reflected from the surface. The ability to probe such an interface has been demonstrated recently[10] and allows, for the first time, the study of a wide range of problems important to material scientists.

Recent work in this group has involved the use of SHG in electrochemical studies of iron passivation.[19-22] SHG studies are extremely sensitive to compositional and electronic changes that occur on the iron electrode as it is cycled. The details of the compositional changes that occur as iron is electrochemically oxidized and reduced are becoming more clear. Additionally, one would like to understand the details of the structure of the oxide layers.

The structure of the oxide layers that form on iron exposed to oxygen has been explored in UHV.[23-33] Several low-energy electron diffraction (LEED) studies have determined the symmetry of thin (less than a monolayer) oxygen overlayers on iron single-crystal faces. Two distinct structures are observed for submonolayer coverages of adsorbed oxygen. Initially, a $c(2\times2)$ overlayer is observed, which transforms at elevated temperatures to a hexagonal structure. Upon further oxidation, no pattern is observed in LEED studies.[23] The iron oxide/vacuum interface is clearly amorphous after significant oxygen dosing, but this does not preclude the possibility of structure in the oxide near the iron interface.

In light of the UHV results, questions remain concerning the structure of air-formed oxide. Is the entire oxide layer amorphous, or does structure persist at the Fe–oxide interface? If structure does persist in the chemically bonded oxygen lattice, is it the same structure as observed for low coverages of adsorbed oxygen? With the use of SHG as a structure-sensitive analytical tool, these questions can be addressed for the interface responsible for iron passivation.

In this report preliminary results of AR-SHG studies of air-oxidized Fe (110) surfaces are described. The observation of a nearly 3-fold pattern in the SHG data is the first clear indication of structure in the air-formed oxide on iron. Bilateral symmetry similar to that expected for the underlying iron substrate is also observed. The implications of these results on the understanding of iron passivation are discussed.

Experimental Section

Samples were cut from a commercially obtained single crystal and oriented by Laue backscattering to within ±0.5°. The surface was ground with 600 grit silicon carbide abrasive, etched for 2.5 min with 5% nitric acid in ethanol to regain surface crystallinity, and then polished with 5-μm and then 1-μm diamond paste and finally with 0.05-μm alumina. This procedure produced a surface of optical quality with no observable polishing scratches and good surface crystallinity as observed by Laue backscattering. Subsequent LEED studies of this sample with this preparation scheme exhibited a sharp (1×1) pattern after sputtering at 600 °C to remove air-formed oxide in agreement with the work of other groups.[32]

The laser, optics, and photon-counting system have been described previously.[19] A Spectra Physics Nd:YAG laser modelocked and Q-switched at 1 kHz is used to produce 100-ps pulses. The use of Q-switched, picosecond pulses is necessary to produce adequate signals from poor second harmonic generators such as iron surfaces. The IR fundamental of the Nd:YAG (1.06-μm wavelength) was used as the incident beam in this study. The laser was focused to a 100-μm-diameter spot on the electrode. The peak laser intensity is on the order of 1 GW/cm^2, which is within an order of magnitude of the damage threshold of the material. No surface damage was observed in these experiments, but modifications of the surface due to laser heating must be considered.

The laser polarization is controlled by a Fresnel rhomb polarization rotator and a Glan–Taylor polarizer and is either s or p upon interaction with the surface. The detected SHG was always p polarized. In some experiments the detecting polarizer was omitted to improve signal collection. Three input angles were used: 5°, 45°, and 65° from the surface normal.

(2) Grubb, S. G.; DeSantolo, A. M.; Hall, R. B. *J. Phys. Chem.* **1988**, *92*, 1419.
(3) Heuer, W.; Schroter, L.; Zachorias, H. *Chem. Phys. Lett.* **1987**, *135*, 299.
(4) Heskett, D.; Song, K. J.; Burns, A.; Plummer, E. W.; Dai, H. L. *J. Chem. Phys.* **1986**, *85*, 7490.
(5) Tom, H. W. K.; Aumiller, G. D. *Phys. Rev.* **1986**, *B33*, 8818.
(6) Zhu, X. O.; Shen, Y. R. *Surf. Sci.* **1985**, *163*, 114.
(7) Litwin, J. A.; Sipe, J. E.; Van Driel, H. M. *Phys. Rev.* **1985**, *B31*, 5543.
(8) Heinz, T. F.; Loy, M. M. T.; Thompson, W. A. *Phys. Rev. Lett.* **1985**, *54*, 63.
(9) Tom, H. W. K.; Mate, C. M.; Zhu, X. D.; Crowell, J. E.; Heinz, T. F.; Somorja, G. A.; Shen, Y. R. *Phys. Rev. Lett.* **1984**, *52*, 348.
(10) Tom, H. W. K.; Heinz, T. F.; Shen, Y. R. *Phys. Rev. Lett.* **1983**, *51*, 1983.
(11) Miragliotta, J.; Furtak, T. E. *Phys. Rev.* **1988**, *B37*, 1028.
(12) Shannon, V. L.; Koos, D. A.; Richmond, G. L. *Appl. Opt.* **1987**, *26*, 3579.
(13) Koos, D. A.; Shannon, V. L.; Richmond, G. L., submitted to *J. Chem. Phys.*
(14) Shannon, V. L.; Koos, D. A.; Richmond, G. *J. Phys. Chem.* **1987**, *91*, 5548.
(15) Shannon, V. L.; Koos, D. A.; Robinson, J. M.; Richmond, G. L. *Chemically Modified Surfaces*; Gordon and Breach Science Publishers: New York; Vol. 2, in press.
(16) Shannon, V. L.; Koos, D. A.; Richmond, G. L. *J. Phys. Chem.* **1987**, *87*, 1440.
(17) Shannon, V. L.; Koos, D. A.; Robinson, J. M.; Richmond, G. L. *Chem. Phys. Lett.* **1987**, *142*, 323.
(18) Robinson, J. M.; Rojhantalab, H. M.; Shannon, V. L.; Koos, D. A.; Richmond, G. L. *Pure Appl. Chem.* **1987**, *59*, 1263.
(19) Biwer, B. M.; Pellin, M. J.; Schauer, M. W.; Gruen, D. M. *Surf. Sci.* **1986**, *176*, 377.
(20) Biwer, B. M.; Pellin, M. J.; Schauer, M. W.; Gruen, D. M. *Langmuir* **1988**, *4*, 121.
(21) Biwer, B. M.; Schauer, M. W.; Pellin, M. J.; Gruen, D. M., submitted to *Surf. Sci.*
(22) Schauer, M. W.; Biwer, B. M.; Pellin, M. J.; Frye, J. M.; Gruen, D. M., to be published.
(23) Sewell, P. B.; Stockbridge, L. D.; Cohen, M. *J. Electrochem. Soc.* **1961**, *108*, 933.
(24) Pignollo, A. J.; Pellissier, G. E. *J. Electrochem. Soc.* **1965**, *112*, 1188.
(25) Shih, H. D.; Jona, F.; Jepsen, D. W.; Marcus, P. M. *Surf. Sci.* **1981**, *104*, 39.
(26) Sewell, P. B.; Mitchell, D. F.; Cohen, M. *Surf. Sci.* **1972**, *33*, 535.
(27) Legg, K. O.; Jona, F.; Jepsen, D. W.; Marcus, P. M. *Phys. Rev.* **1977**, *B16*, 5271.
(28) Simmons, G. W.; Dwyer, D. J. *Surf. Sci.* **1975**, *48*, 373.
(29) Brucker, C. F.; Rhodin, T. N. *Surf. Sci.* **1976**, *57*, 523.
(30) Pirug, G.; Broden, G.; Bonzel, H. P. *Surf. Sci.* **1980**, *94*, 323.
(31) Leygraf, C.; Ekelund, S. *Surf. Sci.* **1973**, *40*, 609.
(32) Langell, M.; Somorjai, G. A. *J. Vac. Sci. Technol.* **1982**, *21*, 858.
(33) Brundle, C. R. *Surf. Sci.* **1977**, *66*, 581.

The random error in the SHG signal was typically within a factor of 2 of the shot noise limit (1–4% of the SHG intensity). Long-term drifts in the laser power were corrected by dividing the SHG intensity by a reference signal generated in calcite. Despite this correction, slow changes in the SHG intensity were often observed for the first 20 min or so of laser irradiation of a freshly polished sample. These changes typically increased the signal at 0° by 10–20% and may be due to laser heating.

Theory

The SHG intensity as a function of the angle of rotation of the crystal surface about the surface normal will reveal the symmetry of the surface. In this study the (110) surface of iron (body-centered cubic) was studied. This surface has bilateral symmetry; therefore, the SHG pattern from such a surface should exhibit two orthogonal mirror planes of symmetry.

The observed SHG patterns (presented in the following section) revealed both 2-fold and 3-fold symmetry. Furthermore, the 3-fold patterns have a pronounced asymmetry. Current theory dealing with angularly resolved SHG considers surfaces of bulk material with cubic symmetry rotated about the surface normal.[34] The existing theory will not describe an asymmetric pattern arising from the rotation of a cubic crystal surface about its normal.

The observed asymmetry in the 3-fold pattern could arise from the formation of an oxide overlayer with 3-fold symmetry forming an imperfect fit with the 2-fold symmetric iron substrate. UHV results have suggested that of the three major faces of FeO, the (111) face has the best fit to the (110) face of iron.[23] Furthermore, oxygen is known to form a hexagonal overlayer under certain conditions at low coverages.[30-32] Therefore, it does not seem unreasonable to suggest that the 3-fold symmetry observed in the SHG pattern is due to the air-formed oxide on the iron surface. The existing theory will, therefore, be extended to include overlayers tilted with respect to the surface normal.

To model the asymmetry of the SHG patterns, we fit the data to a function derived from the expressions describing a cubic (111) face.[34] The induced polarization for a p-polarized fundamental and p-polarized SHG is given by

$$P(2\omega) = [A + C \cos 3(\phi - \beta)]E^2(\omega) \quad (1)$$

where β is an angular displacement relative to an external axis. The observed SHG intensity is proportional to the square of the induced polarization. The coefficients A and C are the isotropic and anisotropic contributions to the SHG and are functions of the incident angle of the fundamental and the exit angle of the SHG signal. These coefficients are given explicitly in terms of microscopic tensor elements in ref 34.

The principal effect of a tilt in the crystal axis relative to the surface normal is to change the effective incident and exit angles. To model this tilt, we write the coefficients A and C in terms of incident angle θ and exit angle θ'. These angles are then changed by an amount related to the tilt angle (δ), the orientation of the tilt (γ), and the orientation of the crystal in the laboratory frame (ϕ). Two assumptions were made to simplify the expression. The exit angle with respect to the surface is assumed to be equal to the incident angle. Also, the surface contribution to C is assumed to dominate over the bulk contribution at incident angles of 65° and 45°. The angles describing this model are summarized in Figure 1.

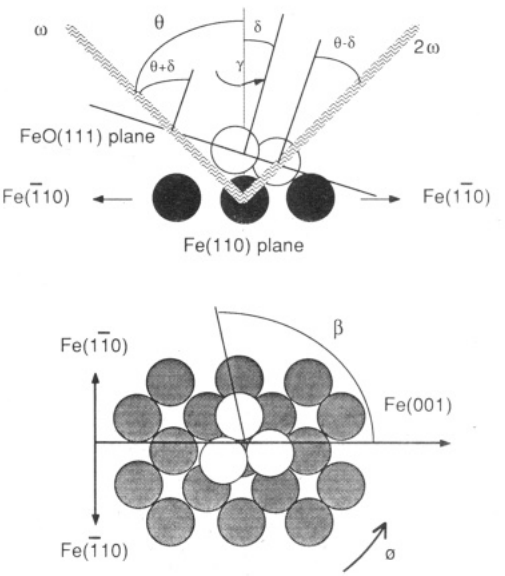

Figure 1. Top: oxygen atoms in the FeO (111) plane (shaded circles) tilted by an angle δ with respect to the Fe (110) plane (black spheres). The orientation of the tilt with respect to the Z axis of the substrate is given by γ. The incident laser makes an angle θ with respect to the substrate normal, and the angle of SHG generation is assumed to be the same as the incident angle. The incident beam makes an angle $\theta + \delta$, and the SHG beam makes an angle $\theta - \delta$ with respect to the FeO (111) axis. Bottom: β, the angle between the Fe (001) axis, and the projection of the (001) direction of the FeO film onto the Fe (110) substrate.

With these assumptions the isotropic and anisotropic coefficients for a tilted (111) overlayer as observed with p-incident and p-detected beams can be written as[34]

$$A_{pp} = i\Omega[\zeta_{31}(F_s - F_s f_s^2) + \zeta_{33}(F_s - F_s f_s^2) - \zeta_{15}F_c f_c f_s] \quad (2)$$

$$C_{pp} = -i\Omega\zeta_{11}F_c f_c^2 \quad (3)$$

where $i\Omega\zeta$ is a component of the surface nonlinear susceptibility. The tilt can be introduced by writing the incident Fresnel coefficients as

$$f_c = \cos\{\theta - \delta[\cos(\phi - \gamma)]\} \quad (4)$$

$$f_s = \sin\{\theta - \delta[\cos(\phi - \gamma)]\} \quad (5)$$

and the detected beam Fresnel coefficients as

$$F_c = \cos\{\theta + \delta[\cos(\phi - \gamma)]\} \quad (6)$$

$$F_s = \sin\{\theta + \delta[\cos(\phi - \gamma)]\} \quad (7)$$

The SHG pattern observed with an incident angle of 65° was fitted by using a seven-parameter least-squares routine where the seven parameters are related to ζ_{31}, ζ_{33}, ζ_{15}, ζ_{11}, δ γ, and β. For the data taken with an incident beam at 45°, ζ_{33} and ζ_{15} are not distinguishable.

The 3-fold pattern observed with an incident angle of 5° was obtained with s-incident polarization. The isotropic and anisotropic terms for this geometry are given by

$$A_{sp} = i\Omega\zeta_{31}F_s \quad (8)$$

$$C_{sp} = i\Omega\zeta_{11}F_c \quad (9)$$

$$B_{sp} = \tfrac{2}{3}\Gamma[(2F_s f_c + F_c f_s) + 2(F_c f_c + F_s f_s)\cos 3(\phi - \beta)] \quad (10)$$

where B is the bulk contribution.

The SHG patterns observed with p-incident and p-detected beams at 5° incident angle show the bilateral symmetry expected from a (110) surface. Whether the observed pattern originates from the Fe (110) surface or a

(34) Sipe, J. E.; Moss, D. J.; Van Driel, H. M. *Phys. Rev.* **1987**, *B35*, 1129.

Table I. Parameters for the Least-Squares Fit to the Tilted (111) Model of SHG from Air-Oxidized Fe (110) (See Text) for Various Incident Angles[a]

θ, deg	ζ_{11}[b]	ζ_{15}	ζ_{31}	ζ_{33}	β	δ	γ[d]	B/C
65	1.00	4 (3)	0.7 (5)	1 (1)	90 (1)	6 (2)	202 (1)	
45	1.00	1 (1)	2.0 (2)	1[c]	93 (1)	5 (2)	237 (1)	
5	1.00		0.61 (3)		89 (1)	3 (1)	230 (6)	1.08 (1)

[a] The fits are plotted with the data in Figure 2. β, δ, and γ are given in degrees. The surface coefficients are relative to ζ_{11}. [b] ζ_{11} is set equal to 1. [c] Value for ζ_{33} is assumed for calculation of ζ_{15}. [d] Due to the small tilt angle, the accuracy of the orientation of the tilt may be larger than the stated uncertainty.

commensurate oxide layer, a pattern with this symmetry should be modeled by using the (110) symmetry equations in ref 34 untilted. In this case, the fresnel coefficients are simply the sine and cosine of the incident angle, and the SHG intensity can be written as

$$I(2\omega) = \{B + C[A + \cos 2(\phi - \beta)]\}^2 \qquad (11)$$

where the bulk term B is given by

$$B = \Gamma\{5/4 + 2 \cos 2(\phi - \beta) + 3/4 \cos 4(\phi - \beta)\} \qquad (12)$$

Four parameters are used in this fit (A, B, C, β), although β should be equal to zero.

From the theory of Sipe et al.,[34] the intensity of the anisotropic contribution is expected to be nearly zero for a surface with nearly 4-fold symmetry, as is the case with the Fe (110) surface, if the incident beam is s polarized. By contrast, the (111) surface intensity in such an experiment is expected to be relatively large. This explains the 3-fold symmetry of the pattern observed with s-polarized incident light.

In the p polarized experiment with $\theta = 5°$, there is no cancellation of the (110) intensity for nearly 4-fold symmetric surfaces. Although the (110) surface contribution is expected to go to zero as θ goes to zero, significant observable intensity can be expected at $\theta = 5°$. On the other hand, for the (111) surface, interference effects between the surface and bulk terms could significantly reduce the observed SHG from this geometry by using p polarized light.

Due to the large numbers of parameters used in these fits, the solutions to the least-squares routine are not unique. By controlling the starting parameters, it is possible to find the best fit to the data rather than a local optimum. The fact that the best fits to the data produced physically meaningful parameters that are consistent throughout this series of experiments instills some confidence in the results.

The selection of the positive direction of the Z axis of the iron substrate is arbitrary since the Fe (110) surface has a mirror plane of symmetry perpendicular to the Z axis. The oxide may select one of two possible equivalent orientations of its 3-fold axis with respect to the surface substrate. This selection occurs through slight asymmetries inevitably present during crystal orientation and surface preparation. A misalignment of 0.5° would produce a step density of about 1%. If oxide growth originates from steps, one orientation may predominate.

Results and Discussion

The nearly 3-fold symmetry of the rotationally resolved SHG pattern of air-oxidized Fe (110) is clearly visible by using an incident angle of 5° (Figure 2a). The asymmetry of the 3-fold symmetric structure with respect to the surface normal is more clearly evident as the incident angle is increased to 45° (Figure 2b) and 65° (Figure 2c). A least-squares fit to the model described above indicates a tilt δ of about 5° (see Table I). This should be considered an estimate with an uncertainty of ±2°. While β (the orientation of the projection of the overlayer (001) axis onto the substrate, with respect to the substrate (001) direction) is determined fairly precisely in these fits (±1°), the uncertainty in γ (the orientation of the tilt) is very large (±20°). The relative values of the surface tensor elements should be considered accurate to within 50%.

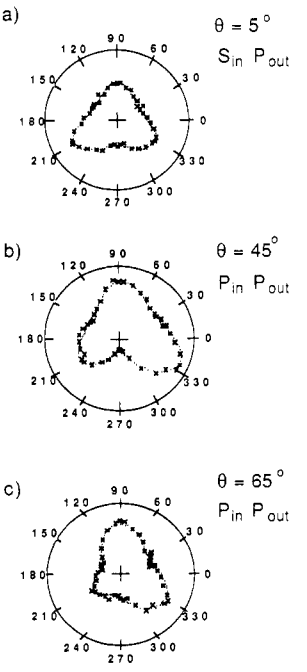

Figure 2. SHG intensity plotted as a function of rotation of the Fe (110) surface about its normal. The Fe (001) direction is taken as 0°. In plot a, the incident beam is s polarized and $\theta = 5°$ from the surface normal. In plot b, the incident beam is p polarized and $\theta = 45°$. In plot c, the incident beam is p polarized and $\theta = 65°$. The small dots plot a least-squares fit to a tilted (111) overlayer on the Fe (110) surface. The parameters for the least-squares fit are given in Table I. Random error in the SHG data is approximately given by the size of the dots in the theory plot.

The orientation of the 3-fold pattern can be understood by modeling the interface with three atoms of the FeO (111) face in contact with an Fe (110) substrate. If the three surface atoms are centered on a substrate atom, the observed orientation indicates that one of the surface atoms (A) would point perpendicularly to the (001) direction of the substrate. This would place atom A in close contact with three substrate atoms, while atoms B and C would be in close contact with two substrate atoms. The asymmetry of this surface/substrate interaction could give rise to the observed tilt in the (111) overlayer symmetry. Considering the entire surface, the tilting of small domains in some average direction would produce kinks, or steps, in the surface, thus limiting the effectiveness of the substrate passivation by the (111) overlayer.

The intensities plotted in Figure 2 are normalized to the square of the laser power and are arbitrary between experiments. In general the signal intensity decreases with decreasing incident angle for p-polarized incident radiation

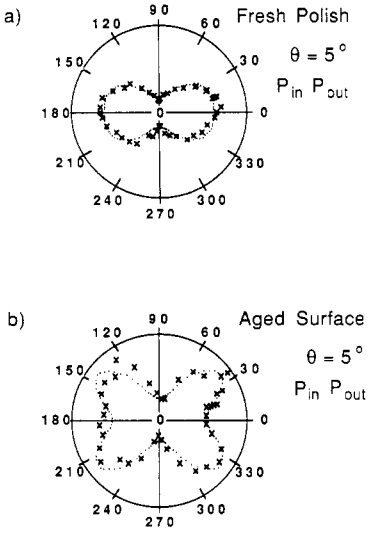

Figure 3. SHG intensity plotted as a function of rotation of the Fe (110) surface about its normal. The Fe (001) direction is taken as 0°. The incident beam is p polarized and 5° from the surface normal. The upper curve represents data obtained immediately after polishing and shows a surface with the bilateral symmetry of the underlying (110) surface. The lower curve shows the same surface several hours later as bulk (110) symmetry develops. Random error in the SHG data is approximately given by the size of the dots in the theory plot.

Table II. Parameters for the Least-Squares Fit of SHG Data in Figure 3 to a Model for a Surface with (110) Symmetry[a]

	ζ_{15}[b]	ζ_{24}	ζ_{31}[b]	β	B/C
fresh polish	2	1 (1)	0.6	1 (1)	0.14 (2)
aged surface	2	1 (1)	0.6	−3 (1)	0.37 (2)

[a] β is given in degrees. B/C is in arbitrary units and should not be compared to B/C in Table I. [b] Values assumed for the calculation of ζ_{24}.

due to terms involving sin θ in eq 1.

Using a p-polarized incident beam with an incident angle of 5°, the 3-fold contribution to the SHG signal has dropped to the point where a pattern with bilateral symmetry is observed (Figure 3). Immediately after polishing (within half an hour), the observed pattern features two lobes. This pattern changes slowly with time, and the next day the same sample exhibits a four-lobed pattern. These patterns can be modeled with eq 11 and 12. Both patterns are found to have the same value of the surface coefficient parameter A (eq 11). The difference between the two patterns is the relative contributions from the bulk term as shown in Table II. The initial pattern has virtually no contribution from the bulk term, whereas the older surface is modeled with a large B/C ratio.

Further evidence for a slow change in the oxide layer with time was observed at an incident angle of 45°. While the data presented in Figure 2 are reproducible and stable, occasionally 2-fold symmetric patterns were observed in the 45° experiment immediately after polishing. These 2-fold patterns were not stable with time and sometimes transformed into highly asymmetric 3-fold patterns. Several experimental variables could account for variations in the observed patterns. The differences could be caused by errors in polishing alignment, variations in sample handling after polishing, or differences in laser intensity. While it is clear that the slow kinetics of the oxide transformations can be studied by this technique, this initial study did not control some of the key parameters involved in the transformation. More controlled studies are in progress.

In a complex layered system such as air-oxidized iron, SHG signal can conceivably arise from several sources. The signal could arise from the oxide/air of the metal/oxide interface. Also, the signal could come from iron or from various oxide species. Experiments in UHV systems and the use of tunable lasers could help identify the source or sources giving rise to the observed signal. In the absence of further experimental evidence, however, some preliminary conclusions can be drawn as to the source of SHG signal in these studies.

The nearly 3-fold symmetric patterns most likely arise from an FeO-like oxide at the metal/oxide interface. The hexagonal patterns observed in LEED experiments with low dosages of oxygen support the conclusion that 3-fold patterns should arise from oxides at the metal surface. The (111) surface of FeO (fcc) exhibits the best fit to the Fe (110) surface (bcc); therefore, the incommensurate ordered oxide is described as FeO (111). The bulk oxide is known to be amorphous; therefore, it seems unlikely that the oxide/air interface could produce 3-fold patterns. One might expect, however, an isotropic background due to SHG from the oxide/air interface. A parameter that describes an isotropic background was added to the fitting function. The resulting fit gave aphysical (negative) values to this parameter and did not improve the fit to the data. Apparently the oxide/air interface does not contribute to the observed signal in these experiments.

The patterns exhibiting bilateral symmetry may be arising from the metal surface or a commensurate oxide. The fact that the bulk contribution builds in slowly with time indicates that it is probably related to oxidation. A bulk term due to iron would be expected to remain constant or decrease with oxidation since the bulk iron has not been perturbed from equilibrium in the sample preparation. The fact that the modeled intensities in both the two-lobed and four-lobed patterns give similar values for the relative tensor terms suggests that both patterns arise from the same bonding system. The slow building in of the bulk contribution may be due to migration of oxygen into the bulk iron and may be assisted by laser heating.

Conclusion

Angularly resolved SHG has provided, for the first time, structural information about the iron/oxide interface in air oxidized iron. The nearly 3-fold symmetric SHG pattern observed for an air-oxidized Fe (110) surface suggests the formation of (111) crystallites of iron oxide at the metal interface, below the amorphous oxide surface. The asymmetry of the 3-fold pattern indicates a systematic misfit, or reconstruction of the Fe/FeO interface, to produce an apparent tilt of the 3-fold axis relative to the surface normal. From a least-squares fit to a model, the average tilt was found to be about 5° from the surface normal. This tilt and the resulting steps such a tilt would induce could explain the relatively poor passivation of iron. A commensurate oxide was also observed. This structure changes with time and may indicate migration of oxygen into the bulk. Work is in progress to extend these measurements to UHV and electrochemical environments.